Semiclassical theory of Rydberg-wave-packet interferometry

Mark Mallalieu* and C. R. Stroud, Jr.
The Institute of Optics, University of Rochester, Rochester, New York 14627
(Received 28 June 1994)

A semiclassical approximation is derived for the autocorrelation function describing the excitation and detection of Rydberg wave packets by pairs of phase-locked laser pulses. The resulting expression is in terms of a sum over Kepler trajectories, and provides a direct explanation of the periodicity and spreading of the wave packet at short times when the evolution is classical. More surprisingly, this solution also provides an accurate description of the complex revival behavior of the wave packets, which is nonclassical. The phases of the wave packets, which are detected by the pulse-locking scheme, are also accurately given by analytical expressions derived from the semiclassical sum. The phases of the wave packets at short times have a simple interpretation as the phases of Bohr-Sommerfeld, and are related to Berry's phase. The semiclassical expression for the phases of the nonclassical revival wave packets is simpler than the corresponding quantal solution.

PACS number(s): 03.65.Sq, 32.80.Rm

I. INTRODUCTION

Wave-packet states in Rydberg atoms are a matter of current experimental and theoretical study, due to their usefulness for studying the classical limit. Such states are deemed quasiclassical because the uncertainty in one or more coordinates of the electron can be reduced to close to the minimum value, leading to subsequent behavior that has many characteristics in common with the classical system. The simplest of these states is the radial wave packet excited with a short laser pulse with no other external fields present [1–7]. These states are well localized in the radial coordinate due to the superposition of many eigenstates with different principal quantum numbers. However, they are not localized in the angular variables because the states in the superposition all have the same angular momentum. This can be overcome by using external fields to mix the angular states. An example of this is the angularly localized wave packet [8] that is excited with a laser pulse in conjunction with a radio frequency field. These wave packets are localized only in the angular variables as the states in the superposition all have the same principal quantum number. A method to prepare a wave-packet state well localized in all three dimensions has been proposed by Gaeta *et al.* [9].

The primary issue regarding these quasiclassical states is the relationship between their dynamics and some underlying set of classical trajectories. The ionization of the angularly localized wave packet studied by Yeazell and Stroud [8] was properly accounted for by modeling the ionization of an ensemble of Kepler trajectories with the same energy and angular distribution as the wave packet. Turning this approach on its head, Gaeta *et al.* [9] developed a method to create three-dimensionally localized wave packets by considering the effects of a short electric pulse on an ensemble of circular orbits intended to model the initial circular-orbit eigenstate. The common feature in both of these models is that the dynamics of the ionization process and wave-packet formation, respectively, occurred on a relatively short time scale. The dynamics of the radial wave packets, as well as wave packets localized about a circular [10] or elliptical [11] orbit, can also be understood on short time scales by using an ensemble of classical trajectories with the appropriate initial conditions. For a number of orbital periods all of the trajectories remain close to one another as they travel around their Kepler ellipses, except when they approach close to the nucleus where small differences in initial conditions are magnified. However, this model breaks down at longer times because small initial uncertainties in position grow with time due to the nonlinearity of the Coulomb potential. After a number of classical periods, the wave packet spreads so much that it is delocalized about the classical orbit, and quantum mechanical interference effects become important [10–12]. These interference effects can be accounted for with the use of sums over classical-path amplitudes [13,14], maintaining the close connection between the wave-packet dynamics and the corresponding classical ensemble.

A most interesting phenomenon occurs at times when the delocalized wave-packet state revives back into a well-defined wave packet, or into a set of symmetrically distributed wave-packet replicas [10,12]. The revivals into multiple copies of the initial wave-packet state occur at certain fractions of the period for a full revival, and thus are called fractional revivals. During these fractional revivals, the wave function consists of a macroscopic superposition of identical wave-packet states which are distinguishable. The coherence between these fractional revival wave packets can be expressed by the superposition coefficients which have been calculated by Averbukh and Perelman [12]. The phases of these amplitudes

*Present address: Department of Chemistry, University of Kansas, Lawrence, KS 66045.

can be measured using sequences of phase-locked pulses [15]. This technique involves a wave-packet interferometry [16,17]. The various laser pulses excite identical wave packets at different times, and the interference among the wave packets determines the final signal. The nature of the interference depends upon the evolution of the first wave packet during the time before the second pulse arrives, and upon the phase relationship between the two pulses. It is this dependence on the optical phase which can be used to measure the fractional wave-packet phases [18,19].

One of the purposes of this paper is to relate these fractional wave-packet phases to the properties of the relevant classical trajectories. This is accomplished with a semiclassical theory based on the classical-path representation (CPR) of Alber and Zoller [1,3,20]. This method is useful for studies of Rydberg wave packets excited from the ground state by short laser pulses, because it includes the effects of laser polarization and the nonhydrogenic quantum defects in alkali-metal atoms in a natural way. In Sec. II, we derive the CPR of the phase-locked pulse process. This is used in Sec. III to show that the phase of the wave packet as it evolves at short times can be related to the classical action of the mean-energy trajectory while the wave packet remains well localized. A solution for the semiclassical sum which is accurate for long times is next obtained in Sec. IV, providing a basis for investigation of the fractional revivals. This solution is similar to that obtained for the autocorrelation function of one-dimensional [13] and three-dimensional circular-orbit Rydberg wave packets [14], which use the semiclassical theory of Tomsovic and Heller [21]. Analysis of the accurate sum in Sec. V reveals that the fractional revivals are correlated with discrete sets of Kepler orbits. This relationship between the various sets of orbits and the different wave-packet fractions includes the locations of the peaks and their phases. We show how the probe laser pulse can be adjusted to selectively emphasize one or another of the fractional wave packets.

II. CPR FOR PHASE-LOCKED PULSE MEASUREMENTS

The classical path representation is discussed extensively in the review of Alber and Zoller [1]. Their general theory handles more complex alkali atoms as well as hydrogen, and the extension of the following analysis to those cases is straightforward. This semiclassical approach has been used previously to treat Raman transition pump-probe processes. In that case, the response is proportional to the magnitude of a semiclassical sum. We apply the method here to a pump-probe process which uses identical pump and probe pulses. This *phase-sensitive* pump-probe process has some advantages with regards to the signal obtainable in experiments, provided that the relative phase between the two pulses is properly controlled. When this is implemented by using pairs of phase-locked pulses, the evolution of the phase of the wave packet can be measured. In the sections following this one, we show that this phase has an interesting connection to the semiclassical dynamics of the wave packet. First, we give the results of this measurement technique, then we derive its classical-path representation.

We consider excited states created by laser pulses which are tuned from the atomic ground state $|g\rangle$ to an energy $\bar{\varepsilon}$ in the Rydberg series. If the laser pulse is much shorter than the classical period of a classical electron with energy $\bar{\varepsilon}$, a number of Rydberg states $|n\rangle$ are excited. This can been seen from the fact that the energy level spacing of the Rydberg levels is inversely related to the Kepler period of a classical electron at that energy. For a laser pulse which arrives at time t_1, the excited wave packet is accurately represented by

$$\psi_{\rm WP}(\mathbf{r},t,t_1) = i\exp(i\omega_p t_1)\exp(-i\bar{\varepsilon}t)\sum_n \Omega_n F(\delta_n) \times\varphi_n(\mathbf{r})\exp[-i\delta_n(t-t_1)]\ , \tag{1}$$

provided that the pulse is weak in the sense that most of the population remains in the ground state. The Rydberg wave functions are given by $\varphi_n(\mathbf{r}) = \langle \mathbf{r}|n\rangle$. The carrier frequency of the laser pulse is denoted by ω_p, and peak field strength and polarization are given by the vector $\boldsymbol{\xi}_0$. The matrix elements of the field interaction between the ground and excited states are designated by the Rabi frequencies $\Omega_n = \langle n|\mathbf{d}\cdot\boldsymbol{\xi}_0|g\rangle$, where $\mathbf{d}$ is the dipole operator. The Fourier transform of the laser pulse envelope $f(t)$ is given by $F(\delta_n)$, and $\delta_n = \varepsilon_n - \bar{\varepsilon}$ is the difference between the mean energy $\bar{\varepsilon} = \omega_p + \varepsilon_g$ and the energy levels $\varepsilon_n = -1/(2n^2)$ (atomic units).

A second laser pulse, identical to the first, arrives at time t_2 and excites another wave packet which is the same as the first wave packet, except for the evolution of the first wave packet and a phase factor which accounts for the optical phase difference between the pulses. The final population in the Rydberg series after the second pulse has passed depends upon the interference between the two wave packets. This population can be measured with a swept electric field that ionizes all excited states. The measured population is $P(t_d) = P_{\rm ave} + P_C(t_d)$, which depends only on the delay between the two pulses, $t_d = t_2 - t_1$, not the absolute times t_1 and t_2. The average population $P_{\rm ave}$ is the incoherent sum of the population of the two wave packets and the interference population P_C depends on the interference between the two wave packets. Details of the calculation will be published elsewhere [15], we give the important results here. Assuming that the two laser pulses are phase locked, the contribution to the population due to the interference of the two wave packets is given by $P_C(t_d) = P_{\rm ave}C_L(t_d;\varepsilon_{g\ell};\phi_\ell)$, with the *phase-locked autocorrelation function* defined by

$$C_L(t_d;\varepsilon_{g\ell};\phi_\ell) = \mathrm{Re}\left\{C(t_d;\varepsilon_{g\ell})\exp(-i\phi_\ell)\right\}. \tag{2}$$

Here ϕ_ℓ is the relative phase difference at which the two laser pulses are locked and ω_ℓ is the frequency at which the phase is locked. This frequency does not need to coincide with ω_p, but is assumed to be within the laser bandwidth. The phase-locked autocorrelation function depends on the optical phase ϕ_ℓ and the autocorrelation

function of the wave packet in the rotating frame at $\varepsilon_{g\ell} = \omega_\ell + \varepsilon_g$,

$$C(t_d;\varepsilon_{g\ell}) = \frac{\langle\widetilde{\Psi}_{\rm WP}(0;\varepsilon_{g\ell})|\widetilde{\Psi}_{\rm WP}(t_d;\varepsilon_{g\ell})\rangle}{\langle\widetilde{\Psi}_{\rm WP}(0;\varepsilon_{g\ell})|\widetilde{\Psi}_{\rm WP}(0;\varepsilon_{g\ell})\rangle}. \quad (3)$$

The wave packet in the rotated frame is given by

$$\widetilde{\psi}_{\rm WP}(\mathbf{r},t;\varepsilon_{g\ell}) = i\sum_n \Omega_n F(\delta_n)\varphi_n(\mathbf{r})\exp[-i(\varepsilon_n-\varepsilon_{g\ell})t]\,. \quad (4)$$

It would seem natural to choose the rotated frame to be at $\bar{\varepsilon}$, but as we shall see in Sec. V there are other appropriate rotated frames. The peaks of the autocorrelation function in Eq. (3) have the same form as the pulse envelope $f(t)$ so long as the wave packet remains well localized, as we shall see in the next section. However, the phase of the autocorrelation function at its peaks is very sensitive to its mean energy. This phase has a simple semiclassical interpretation, and will also be discussed in the next section.

We now find the classical-path representation [1,3,20] of the phase-locked pulse excitation. Using the resolvent $G^+(\varepsilon) = [\varepsilon - H_a + i0]^{-1}$ in Eqs. (3) and (4), the wave-packet autocorrelation function becomes

$$C(t_d;\varepsilon_{g\ell}) = i(\pi P_{\rm ave})^{-1}\exp(i\varepsilon_{g\ell}t_d)\int_{-\infty}^{\infty} d\varepsilon\,|F(\varepsilon-\bar{\varepsilon})|^2 \times\Sigma(\varepsilon)\exp(-i\varepsilon t_d). \quad (5)$$

The *self-energy* of the initial state $|g\rangle$ is given by $\Sigma(\varepsilon) = \langle g|\mathbf{d}\cdot\boldsymbol{\xi}_0^* G^+(\varepsilon)\mathbf{d}\cdot\boldsymbol{\xi}_0|g\rangle$ and is a two-photon transition matrix element from the perturbation theory of two-photon processes. Although the transition from the ground state to the Rydberg series under consideration is a single-photon transition, the pump-probe process itself is a two-photon process because there is interference between the possibility of an excited state absorbing a photon from the first or second laser pulse. The self-energy is related to the wave function $|U_\varepsilon\rangle = G^+(\varepsilon)\mathbf{d}\cdot\boldsymbol{\xi}_0|g\rangle$ which is seen to satisfy the inhomogeneous Schrödinger equation $(\varepsilon - H_a - i0)|U_\varepsilon\rangle = \mathbf{d}\cdot\boldsymbol{\xi}_0|g\rangle$. Once this equation is solved, the self-energy is readily obtained.

The state $|U_\varepsilon\rangle$ is determined in several steps. At small values of the radius, the wave function is given by Coulomb functions. For atoms with a complex core, the boundary conditions are matched at $r \to 0$ with quantum defect methods [1], whereas for hydrogen a standard Green's function method suffices. At this step the outer boundary condition is satisfied by an outgoing Coulomb wave which takes into account the fact that the wave function is being excited by a laser. At some suitable intermediate radius ($r_c \sim 50a_0$), which is outside the atom-laser interaction region, but still small on the scale of the classical orbits at the energy being considered, the WKB form of the Coulomb functions can be used.

At this point the theory of Maslov and Fedoriuk [22,23], which uses a semiclassical approximation to the Green's function $G(\mathbf{q},\mathbf{q}',\varepsilon)$, can be applied to the propagation of the wave function. An initial manifold of trajectories starting at the surface r_c corresponding to the outgoing Coulomb waves at energy ε is propagated using classical equations of motion [24,25]. The incoming Coulomb waves are then expressed in terms of the semiclassical propagation as a sum of classical-path amplitudes involving trajectories which return to the core. The amplitude of the incoming wave due to a particular trajectory is a product of the amplitude of the initial outgoing wave at the point of departure from the surface r_c and a semiclassical amplitude. This semiclassical amplitude has a magnitude which depends upon the stability of the trajectory versus initial angle of departure from r_c, and represents a density of nearby trajectories. The phase of the semiclassical amplitude depends upon the classical action and Maslov index of the trajectory. The Maslov index is related to the phase accumulated by the wave when it travels thru a caustic point.

The total wave function is then found by matching this incoming wave with the wave function generated by the laser. The self-energy is calculated from this wave function, and is now represented as a sum of classical-path amplitudes. For the case of hydrogen with no external fields, the classical-path representation of the self-energy is

$$\Sigma(\varepsilon) = -i\Gamma(\varepsilon)\frac{\exp[iS_1(\varepsilon)]}{1-\exp[iS_1(\varepsilon)]} = -i\Gamma(\varepsilon)\sum_{k=1}^{\infty}\exp[ikS_1(\varepsilon)], \quad (6)$$

when we restrict the two laser pulses to be well separated from each other. [1] The energy normalized Fermi Golden Rule (FGR) transition rate $\Gamma(\varepsilon)$ is closely related to the density of states and the square of the Rabi frequency Ω_n for energies $\varepsilon \approx \varepsilon_n$. It is a smooth extrapolation of the FGR ionization rate above threshold, and is approximately independent of energy [1]. The classical action of a trajectory at energy ε after one Kepler period is given in atomic units by $S_1(\varepsilon) = \oint \mathbf{p}\cdot d\mathbf{q} = 2\pi\nu$. The action variable ν is related to the energy by $\varepsilon = -1/(2\nu^2)$, and corresponds to the principle quantum number n of the quantized hydrogen atom. This expression has poles for integer $\nu = n$; thus, it can be directly related to Bohr quantization.

The solution for the self-energy in Eq. (6) can now be put into Eq. (5) to get the semiclassical approximation to the autocorrelation function, $C(t_d;\varepsilon_{g\ell}) \approx C_{\rm sc}(t_d;\varepsilon_{g\ell})$. Taking the laser pulse to have the Gaussian form $f(t) = (\pi\tau_p^2)^{-1/4}\exp(-t^2/2\tau_p^2)$ and pulling the FGR transition rate at the mean energy $\Gamma(\bar{\varepsilon})$ out of the integral results in

$$C_{\rm sc}(t_d;\varepsilon_{g\ell}) = \frac{\tau_p}{\sqrt{\pi}}\exp(i\varepsilon_{g\ell}t_d)\sum_{k=1}^{\infty}\int_{-\infty}^{\infty}\exp\left[-(\varepsilon-\bar{\varepsilon})^2\tau_p^2 + iS_k(\varepsilon) - i\varepsilon t_d\right]d\varepsilon\,, \quad (7)$$

where we used $P_{\rm ave} \approx 2\Gamma(\bar{\varepsilon})$. All that remains to be done is to evaluate the integral. This requires making an approximation to the classical action $S_k(\varepsilon) = kS_1(\varepsilon)$. For short times an approximation about the mean energy

of the wave packet is adequate, as we show in the next section. For long times a different approach is needed. We improve upon a previous solution [1,3] that used the stationary-phase method to solve the integral. This alternative approach is similar to the use of reference trajectories to propagate Gaussian wave packets with the semiclassical Van Vleck–Gutzwiller propagator [21], and is accurate for a wider range of parameters than the stationary-phase solution.

III. MEASUREMENT OF THE BOHR-SOMMERFELD PHASES

The Ehrenfest regime of the wave-packet evolution is defined as those times for which the wave packet remains well localized about the trajectory of the Kepler orbit at the mean energy. As the evolution proceeds, the wave packet begins to spread. This spreading corresponds to that of an ensemble of Kepler trajectories with the same energy distribution as the wave packet, and the spreading rate can be accurately determined by a linearization of the dynamics about the trajectory at the mean energy. Furthermore, in this section it will be shown that the phase of the wave packet which is measured by the phase-locked pulse technique, summarized by Eq. (2), has a simple semiclassical interpretation as the classical action of the mean-energy trajectory. This classical action is directly related to the Bohr-Sommerfeld action.

It is only necessary to approximate the classical action of the Kepler orbits with a Taylor series to put the integral in Eq. (7) into solvable form. The expansion of the action about some energy ε_0 is

$$S_k(\varepsilon) \approx S_k(\varepsilon_0) + (\varepsilon-\varepsilon_0)\frac{\partial S_k(\varepsilon)}{\partial \varepsilon} \times|_{\varepsilon=\varepsilon_0} + \frac{(\varepsilon-\varepsilon_0)^2}{2}\frac{\partial^2 S_k(\varepsilon)}{\partial^2 \varepsilon}\bigg|_{\varepsilon=\varepsilon_0} + \cdots . \quad (8)$$

From elementary classical mechanics the first derivative of the action is $\partial S_k/\partial\varepsilon = kT_c(\varepsilon)$, where $T_c(\varepsilon) = 2\pi\nu^3$ is the Kepler period of the orbit at the energy $\varepsilon = -1/(2\nu^2)$. The second derivative of the action is given by

$$\frac{k}{2}\frac{\partial T_c(\varepsilon)}{\partial \varepsilon} = \frac{3}{2}k\nu^2 T_c(\varepsilon) \equiv \zeta_k^2(\varepsilon) , \quad (9)$$

and determines the spreading rate of trajectories for small changes in energy about ε. So long as the wave packet remains well localized, it is valid to use the second-order expansion of the action (8) about the mean energy $\bar{\varepsilon}$ in Eq. (7). This yields a simple Gaussian integral which evaluates to

$$C_{sc}(t_d;\varepsilon_{g\ell}) \approx \exp[i(\varepsilon_{g\ell}-\bar{\varepsilon})t_d]\sum_k \frac{\exp\left[iS_k(\bar{\varepsilon})\right]}{[1-i\zeta_k^2(\bar{\varepsilon})/\tau_p^2]^{1/2}} \times \exp\left(-\frac{[t_d-kT_c(\bar{\varepsilon})]^2}{4[\tau_p^2-i\zeta_k^2(\bar{\varepsilon})]}\right) , \quad (10)$$

This describes a series of peaks centered at multiples of the mean-energy Kepler period, with a spreading rate of the peaks determined by $\zeta_k^2(\bar{\varepsilon})$. This result is compared in Fig. 1 with an accurate integration of the full quantum mechanical expression obtained from Eqs. (3) and (4). As anticipated, this result provides an accurate description of the wave-packet evolution until the wave packet breaks up.

The importance of Eq. (10) is that the phase of a well localized Rydberg wave packet in the classical regime is linked to the classical action $S_k(\bar{\varepsilon}) = 2\pi k\bar{\nu}$. This is a multiple of the Bohr-Sommerfeld action which was used in the old quantum mechanics. The phase due to the Bohr-Sommerfeld action was shown to be an example of Berry's phase [27,28] by Littlejohn [29], who used the generalization of Aharonov and Anandan [30]. As seen from Eqs. (2) and (10), this phase can be measured by the phase-locking technique provided that the pulses are locked at the laser carrier frequency ω_p ($\varepsilon_{g\ell} = \bar{\varepsilon}$) with the relative phase between the pulses locked to $\phi_\ell = 0$. This results in a measurement of the real part of each term in the sum in Eq. (10).

If the laser is tuned to an energy such that $\bar{\nu}$ is integer, the response will appear just as expected based on previous analyses of Raman or ionization inducing probe pulses [1,3,4]. For noninteger $\bar{\nu}$ the response differs remarkably, as shown in Fig. 2. The responses shown at $\bar{\nu} = 100$, 100.25, 100.5, and 100.75 were the result of a full numerical integration of Schrödinger's equation, not Eq. (10). However, the semiclassical result provides a simple way of understanding the results. For $\bar{\nu} = 100.25$ and 100.75 the phase due to the action makes the phase-locked autocorrelation function purely imaginary for the first return to the nucleus, so there is no significant response at $T_c(\bar{\varepsilon})$ at these energies. The small response that is seen is due to the spread of the wave packet. For $\bar{\nu} = 100.5$ the phase-locked autocorrelation function is real and negative, so the total response, which is the sum of the interference population and the average pop-

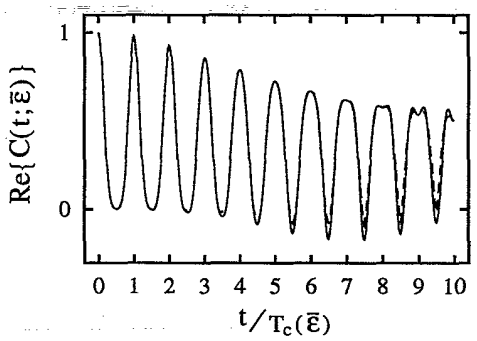

FIG. 1. Accuracy of central-orbit classical-path representation during Ehrenfest regime. The real part of the autocorrelation function for the first ten Kepler periods, for a laser pulse tuned to $\bar{\nu} = 100$ with a pulse length of $\tau = T_c(\bar{\varepsilon})/10$. The solid line is an accurate numerical integration of the time-dependent Schrödinger equation, and the dashed line is the central-orbit classical-path representation.

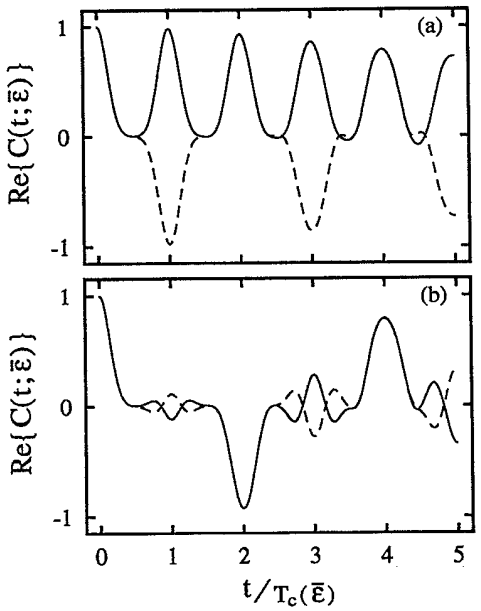

FIG. 2. Wave-packet recurrence peak phase dependence on mean energy. Accurate numerical integration of the autocorrelation function for mean energies corresponding to (a) $\bar{\nu} = 100$ (solid line), 100.5 (dashed line), and (b) $\bar{\nu} = 100.25$ (solid line), 100.75 (dashed line). The dependence of the phase on the central-orbit energy is in complete agreement with that predicted by the semiclassical theory.

ulation, is identically zero. At this energy there will be a sign change every period, which creates the appearance in the response of a wave packet with twice the period that it should have.

Solutions to the classical-path representation obtained by linearizing the dynamics about the mean energy have been used previously to describe the pump-probe response for Rydberg atoms in external fields, using different pump and probe pulses [1,20,26]. In those cases, the nonclassical nature of the semiclassical phases manifests itself when different classical-path amplitudes interfere with one another. This occurs because closed orbits leaving the atomic core at different angles can return to the core at the same time, but having different values of classical action. In light of the results of this section, the phase-locked pulse technique could provide more detail about the properties of such systems. Even in the case of no external fields, however, interferences between different classical-path amplitudes occur. As we see in the next section, this in fact defines the nonclassical regime of the radial Rydberg wave-packet evolution. To investigate that requires a new approach to the solution of the integral in Eq. (7).

IV. MULTIPLE PATHS IN THE NONCLASSICAL REGIME

The breakdown of the solution in Eq. (10) is due to the approximation involved in evaluating the integral Eq. (7), not the semiclassical method itself. The form of this integral suggests the use of the stationary-phase method when t_d becomes large enough, and that is the approach used previously by Alber *et al.* [3] and Alber and Zoller [1]. However, they did not use this result to investigate the fractional revivals of the wave packet, as we shall in the next section. Furthermore, a little reflection on the results of the last section and the relevant classical dynamics leads to an improvement which is good for both long and short times.

The classical analog for the excitation of a wave packet by a laser pulse is obtained by launching a classical ensemble of Kepler electrons from the nucleus, with the starting times of the members of the ensemble distributed about the arrival time of the pulse. The energy distribution of the classical ensemble must also mimic that of the excited wave packet. The classical ensemble spreads as it evolves, due to the variation of the Kepler period $T_c(\varepsilon)$ with energy ε. At long enough times, the faster trajectories will lap the slower ones. At this point the ensemble will be spread entirely about the classical orbit. It makes sense to consider only the subset of trajectories which are in the vicinity of the nucleus when the second pulse arrives, as these are the ones that should be relevant to the response. This follows from the dependence of the response on the wave-packet location when it is still well localized.

The trajectories in the vicinity of the nucleus when the second pulse arrives will be very close to an integer repeat of their periods, so it is useful to account for the contributions of all the trajectories near a given repeat of their periods in terms of the one which exactly repeats its period at time t_d. The kth *reference* trajectory is, thus, determined by the condition $k\mathcal{T}_k = t_d$, where $\mathcal{T}_k = T_c(\varepsilon_k^s)$ is the orbital period of this trajectory. The reference trajectory energies ε_k^s satisfy the stationary-phase condition for the integral in Eq. (7). The action variable of the kth reference orbit is

$$\nu_k = \left(\frac{t_d}{2\pi k}\right)^{1/3} . \tag{11}$$

The classical actions of the nearby trajectories are determined by the Taylor series given in Eq. (8), evaluated at energy ε_k^s. Using this in Eq. (7) and performing the Gaussian integral as in the last section results in

$$C_{sc}(t_d;\varepsilon_{g\ell}) \approx \exp(i\varepsilon_{g\ell}t_d)\sum_k \frac{e^{i\pi/4}}{\eta_k\xi_k}\exp\left(-\frac{(\varepsilon_k^s-\bar{\varepsilon})^2}{\xi_k^2}\right)$$
$$\times \exp\left(i\mathcal{S}_k(t_d) - i\varepsilon_k^s t_d\right), \tag{12}$$

where $\xi_k^2 = 1/\tau_p^2 + i/\eta_k^2$ and $\eta_k^2 = \zeta_k^2(\varepsilon_k^s)$. The classical action of the kth reference orbit is denoted by $\mathcal{S}_k(t_d) = S_k(\varepsilon_k^s)$. We note that the phase in the rightmost exponential is the *full* action $\mathcal{R}_k(t_d) = \int_0^{t_d} dt\mathcal{L}_k = \mathcal{S}_k(t_d) - \varepsilon_k^s t_d$, where $\mathcal{L}_k$ is the Lagrangian of the kth reference orbit. This action plays a role in the time-dependent semiclassical theory used previously [13,14] to calculate the autocorrelation functions of Gaussian wave packets in the Coulomb potential. The result in Eq. (12) is of

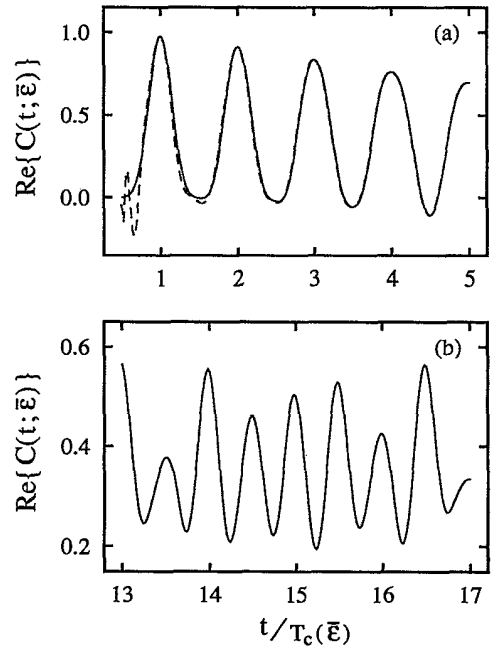

FIG. 3. Accuracy of reference-orbit classical-path representation for a wave packet excited by a long pulse. The real part of the autocorrelation function calculated with the reference-orbit classical-path representation (dashed line) compared to that calculated with an accurate numerical integration (solid line). The laser pulse is tuned to $\bar{n} = 90$ and has width of $\tau = T_c(\bar{\varepsilon})/10$. The times shown are (a) in the Ehrenfest regime (b) near the half revival.

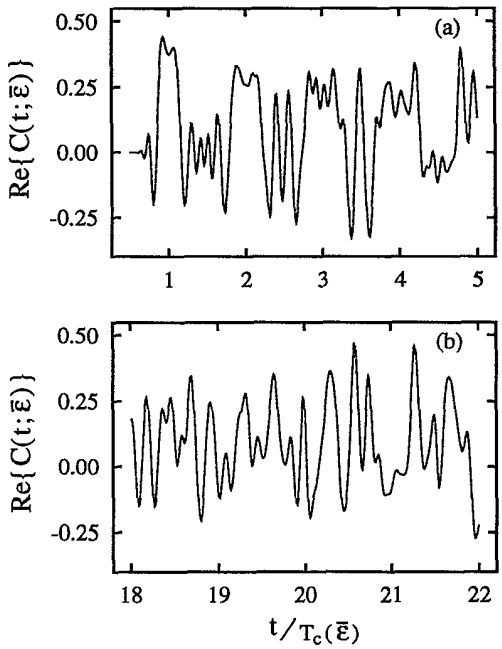

FIG. 4. Accuracy of reference-orbit classical-path representation for a wave packet excited by a short pulse. The real part of the autocorrelation function calculated with the reference-orbit classical-path representation (dashed line) compared to that calculated with an accurate numerical integration (solid line). The laser pulse is tuned to $\bar{n} = 90$ and has width of $\tau = T_c(\bar{\varepsilon})/40$. The times shown are (a) in the Ehrenfest regime (b) near the two-thirds revival.

the same form as those solutions, although the method employed is different. Henceforth, we shall call $\mathcal{S}_k(t_d)$ the *reduced* action, in order to keep the two actions distinct.

The solution in Eq. (12) is compared to the accurate quantum integration in Figs. 3 and 4. Even at the various fractional revivals the semiclassical solution is very accurate. This result can be used to gain insight into the nonclassical regime of the wave-packet evolution. This regime begins when there is more than one significant contribution in Eq. (12). There will then be interference between the classical-path contributions and the quantum probability distribution will differ from a classical distribution. We will show in the next section that the revivals occur at such times that there is complete constructive interference between the terms in the sum in Eq. (12). Such revivals cannot occur for the underlying classical ensemble of trajectories.

In the limit as $t \to \infty$ the condition $\tau_p^2 \ll \eta_k^2$ holds, allowing the approximation $\xi_k \sim 1/\tau_p$. Using this in Eq. (12) yields

$$\begin{aligned} C_{\rm sc}(t_d;\varepsilon_{g\ell}) &\approx C_{\rm st}(t_d;\varepsilon_{g\ell}) \\ &= e^{i\pi/4}\exp(i\varepsilon_{g\ell}t_d) \\ &\quad\times\sum_k \frac{\tau_p}{\eta_k}\exp\left[-(\varepsilon_k^s-\bar{\varepsilon})^2\tau_p^2\right] \\ &\quad\times\exp[i\mathcal{R}_k(t_d)], \end{aligned} \tag{13}$$

which is identical to the stationary-phase solution [1,3] to the integral in Eq. (7). The result given in Eq. (12) is accurate at shorter times and for a larger range of pulse widths than the stationary-phase result in Eq. (13). However, at long times both expressions are indistinguishable from each other or the exact expression in terms of the eigenstate amplitudes. The form (13) will prove useful in the next section for studying the fractional revivals.

V. CORRESPONDENCE BETWEEN FRACTIONAL WAVE PACKETS AND DISCRETE KEPLER ORBITS

The wave-packet evolution is especially nonclassical when it undergoes revivals [10,12], which occur at integer multiples or rational fractions of the revival period,

$$T_{\rm rev} = \frac{\bar{\nu}}{3}T_c(\bar{\varepsilon}). \tag{14}$$

The full actions can be approximated at times near certain fractions of this period such that an explicit evaluation of the semiclassical sum is possible, thereby revealing much about the relationship between the Kepler trajectories and the fractional revivals of the wave packet. As this would take us too far astray, we provide a simpler treatment here which nonetheless illustrates the important features.

The autocorrelation peaks of the revivals at times near some fraction of the revival period, $t_d \approx fT_{\rm rev}$, can be determined by finding the times for which the terms in the semiclassical sum have maximum constructive interfer-

ence. For simplicity, we consider fractions of the revival period such that $f = 1/m_f$, where m_f is an integer. To facilitate the solution for the times of total constructive interference, it is useful to have an expression for the action of each reference trajectory relative to that of one which is close to the mean energy. The first step is to find a time $t_d = k_f T_c(\bar{\varepsilon})$ at which the mean-energy orbit itself is a reference orbit. To keep this time within a Kepler period of the fractional revival time, a convenient choice for the integer k_f is

$$k_f = \left\lfloor \frac{f T_{\rm rev}}{T_c(\bar{\varepsilon})} \right\rfloor = \left\lfloor \frac{\bar{\nu}}{3 m_f} \right\rfloor , \tag{15}$$

where the floor brackets denote the largest integer smaller than the quantity enclosed. For times $t_d \neq k_f T_c(\bar{\varepsilon})$ the mean-energy orbit is not a reference orbit, but the energy of the reference orbit given by $k_f \mathcal{T}_{k_f} = t_d$ is close enough to the mean energy that we can safely expand about it rather than the mean energy, for times within a classical period of $f T_{\rm rev}$.

The action variables ν_k of the nearby reference orbits can be found from that of the k_fth reference orbit with the help of $\mathcal{T}_k = 2\pi\nu_k^3 \approx \mathcal{T}_{k_f}[1 + 3(\nu_k - \nu_{k_f})/\nu_{k_f}]$. This is used along with $k\mathcal{T}_k = k_f \mathcal{T}_{k_f}$ to get

$$\nu_k - \nu_{k_f} \approx -l m_f , \tag{16}$$

where $l = k - k_f$. The assumption $(\nu_k - \nu_{k_f}) \ll \nu_{k_f}$ was used. The expression (16) can be used to get an approximation to the reference trajectory energies ε_k^s by expanding them about $\varepsilon_{k_f}^s$,

$$\varepsilon_k^s - \varepsilon_{k_f}^s \approx (\nu_k - \nu_{k_f}) \frac{2\pi}{\mathcal{T}_{k_f}} - \frac{(\nu_k - \nu_{k_f})^2}{2} \frac{2\pi}{T_{\rm rev}} . \tag{17}$$

The product $(\varepsilon_k^s - \varepsilon_{k_f}^s) t_d$ simplifies using the definition $t_d/\mathcal{T}_{k_f} = k_f$ and the fact that the ratio $t_d/T_{\rm rev} \approx 1/m_f$ does not change significantly for times within a classical period or so of $T_{\rm rev}/m_f$. The action $\mathcal{S}_k = 2\pi k \nu_k$ is easily found in terms of Eq. (16), and after a little algebra we find

$$\mathcal{R}_k(t_d) \approx 2\pi k_f \nu_{k_f} - \varepsilon_{k_f}^s t_d + 2\pi l \left(\nu_{k_f} + \frac{m_f}{2} \right) \pmod{2\pi}. \tag{18}$$

The first two terms on the right hand side of Eq. (18) are independent of l. For maximum constructive interference to occur between the contributions in the sum in Eq. (13), the terms which depend upon l must be a multiple of 2π. This leads to the condition

$$\nu_{k_f} + \frac{m_f}{2} = 0 \pmod 1 . \tag{19}$$

This condition on the reference-orbit action variables for the fractional revival peaks is reminiscent of Bohr quantization for the energy levels. If m_f is even (odd) then ν_{k_f} must be integer (half integer). We call the orbits with action variable an odd multiple of $1/2$ the half-integer orbits, and the orbits with integer action variables are of course the Bohr orbits. Although the role of the Bohr orbits might be expected, the role of the half-integer orbits is perhaps surprising.

In view of Eqs. (19) and (16), the fractional revival peak locations will be more clearly expressed in terms of the periods of a given Bohr orbit near the mean-energy, rather than the periods of the mean-energy itself. The particular Bohr orbit used for the time scale is chosen to be

$$\bar{n} = \lfloor \bar{\nu} \rfloor . \tag{20}$$

Across the interval $k_f T_c(\varepsilon_{\bar{n}}) \leq t_d < (k_f + 1) T_c(\varepsilon_{\bar{n}})$, there are m_f equally spaced times at which the reference orbits will satisfy Eq. (19). This can be seen from the reference orbit spacing given by Eq. (16) and a simple linear extrapolation of the orbits ν_{k_f} across the interval. The fractional revival autocorrelation peaks are centered at

$$t_j = \left(k_f + \frac{\kappa}{2 m_f} + \frac{j}{m_f} \right) T_c(\varepsilon_{\bar{n}}), \qquad j = 0, 1, 2, \ldots, m_f - 1, \tag{21}$$

corresponding to the reference orbits,

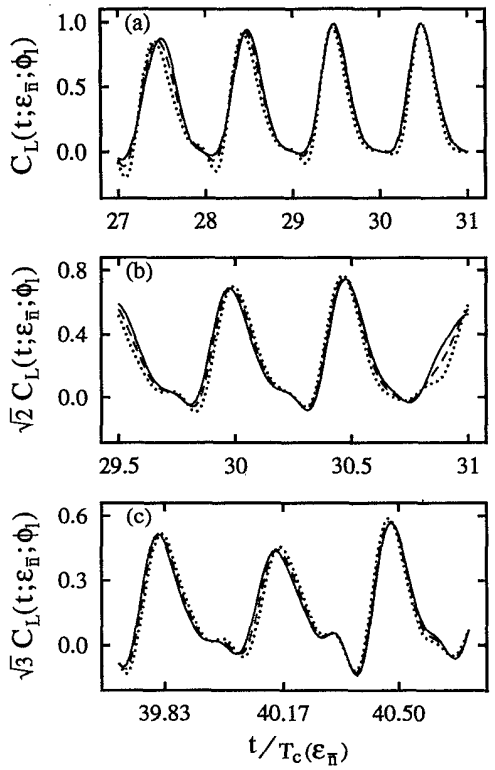

FIG. 5. Insensitivity of revivals to small variations in energy. The real part of the autocorrelation function is shown near the (a) first full revival, (b) one-half revival, (c) one-third revival. In all cases the revival peaks are centered where either the Bohr or the half-integer orbits have a multiple of their orbital period. The mean energies of the curve correspond to (a) $\bar{\nu} = 90$ (solid line), $\bar{\nu} = 90.33$ (dashed line), $\bar{\nu} = 90.67$ (dotted line); (b) $\bar{\nu} = 180$ (solid line), $\bar{\nu} = 180.33$ (dashed line), $\bar{\nu} = 180.67$ (dotted line); (c) $\bar{\nu} = 360$ (solid line), $\bar{\nu} = 3600.33$ (dashed line), $\bar{\nu} = 360.67$ (dotted line).

$$\nu_{jl} = \bar{n} + \frac{\kappa}{2} + j - lm_f \ , \qquad j = 0, 1, 2, \ldots, m_f - 1. \tag{22}$$

The index $\kappa = m_f \pmod 2$ indicates whether it it the Bohr orbits or the half-integer orbits that the peaks are aligned with. For simplicity we have used the time scale $T_c(\varepsilon_{\bar{n}})$ of the mean Bohr orbit even for odd m_f, when the time scale given by $\bar{n} + 1/2$ would be more appropriate.

The revival peaks for the first full revival, the half revival, and the third revival are shown in Fig. 5 for a range of mean energies. The plots show the wave-packet autocorrelation function as determined from an accurate numerical integration of Schrödinger's equation. Regardless of the value of $\bar{n}$, the peaks are centered at times when either the Bohr or the half-integer orbits have a multiple of their orbital periods, in accordance with Eqs. (21) and (22).

Just as the fractional revival peak locations are insensitive to small changes in the mean energy, the phases of the fractional revivals should also be insensitive to small changes in the mean energy. It is best to work in the rotated frame at $\varepsilon_{g\ell} = \varepsilon_{\bar{n}}$ for the phase-locked pulse measurement given in Eq. (2). To get the phase of each fractional revival peak in the appropriate rotating frame, it is necessary to calculate the rotated action $\mathcal{Q}_j \equiv \mathcal{R}_{k_f}(t_j) + \varepsilon_{\bar{n}} t_j$ at each fractional peak time t_j. It has already been shown that all of the reference orbits will have the same actions modulo 2π at these times, so it is simplest to consider the action of the reference orbit with $k = k_f$. Proceeding as before, $\varepsilon^s_{k_f} - \varepsilon_{\bar{n}}$ is expanded as in Eq. (17). The use of Eqs. (21) and (22) results in

$$\mathcal{Q}_j \approx -\frac{\pi}{m_f}\left(j + \frac{\kappa}{2}\right)^2 . \tag{23}$$

To get the total phase of each peak, the phase correction of $\pi/4$ which is present in the stationary-phase result in Eq. (13) needs to be included. This factor comes from the contributions close in energy to the reference orbit. The fractional revival phases are

$$\phi_j = \frac{\pi}{4}\left(1 - \frac{\kappa}{m_f}\right) - \frac{\pi}{m_f}(j + \kappa)j \ . \tag{24}$$

This is a much simpler expression for the fractional revival phases than the corresponding expression which is based on an analysis of the eigenstate amplitudes [12,15]. These phases can be measured by the scheme given by Eq. (2). If the optical phase ϕ_ℓ is equal to the phase of the peak ϕ_j, the measurement will produce a maximum. In [15] we show how this works for the $m_f = 2$ and 3 fractional revivals. Here, we show the $m_f = 4$ revival in Fig. 6 and the $m_f = 5$ revival in Fig. 7. From Eq. (24),

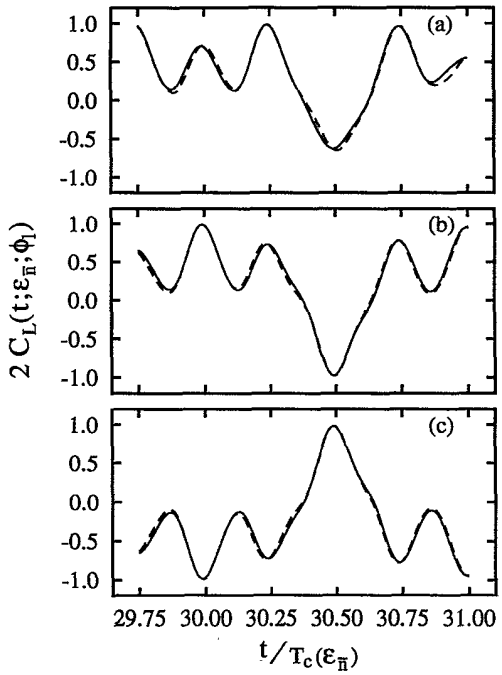

FIG. 6. Phase-locked autocorrelation function at 1/4 revival. The laser pulse is tuned to $\bar{\nu} = 360.0$ (solid line), $\bar{\nu} = 360.5$ (dashed line), with a pulse length of $\tau_p = T_c(\varepsilon_{\bar{n}})/25$. The response is shown for a phase-lock of (a) $\phi_\ell = 0$, (b) $\phi_\ell = \pi/4$, (c) $\phi_\ell = -3\pi/4$. For this revival, the autocorrelation peak phases are given by $\phi_0 = \pi/4$, $\phi_1 = \phi_3 = 0$, and $\phi_2 = -3\pi/4$.

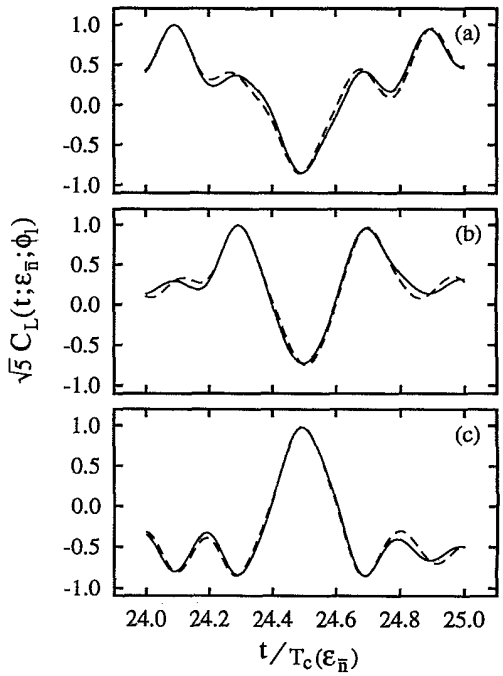

FIG. 7. Phase-locked autocorrelation function at 1/5 revival. The laser pulse is tuned to $\bar{\nu} = 360.0$ (solid line), $\bar{\nu} = 360.5$ (dashed line), with a pulse length of $\tau_p = T_c(\varepsilon_{\bar{n}})/25$. The response is shown for a phase-lock of (a) $\phi_\ell = \pi/5$, (b) $\phi_\ell = -\pi/5$, (c) $\phi_\ell = -\pi$. For this revival, the autocorrelation peak phases are given by $\phi_0 = \phi_4 = \pi/5$, $\phi_1 = \phi_3 = -\pi/5$, and $\phi_2 = -\pi$.

the peak phases of the 1/4 revival are $\phi_0 = \pi/4$, $\phi_1 = \phi_3 = 0$, and $\phi_2 = -3\pi/4$. This is in agreement with the phase-locked autocorrelation function shown in Fig. 6, with the locked-phase set to each of these values. For the 1/5 revival the peak phases are given by $\phi_0 = \phi_4 = \pi/5$, $\phi_1 = \phi_3 = -\pi/5$, and $\phi_2 = -\pi$, which is in agreement with Fig. 7.

VI. CONCLUSIONS

We have found accurate semiclassical solutions during both the classical and quantum regimes of wave-packet evolution. The solution for short times demonstrated that even in the "classical" regime there is a quantum mechanical phase of the wave packet which is a physical observable, as it can be measured by a simple phase-locked laser pulse scheme. This quantum mechanical phase is related to the Bohr-Sommerfeld action of the Kepler orbit at the mean energy of the wave packet. The semiclassical treatment for the wave-packet dynamics in the nonclassical regime is surprisingly accurate. The fractional revival behavior, although an inherently quantum phenomena, is accurately reproduced from interferences among classical-path amplitudes. The various fractional wave packets are seen to correspond to discrete sets of orbits, some of which are Bohr orbits and others which have half-odd values of their action variable. A simple expression for the phases of the fractional wave packets was derived from the semiclassical solution. These phases are directly related to the classical action of the discrete orbits of the fractional revival wave packets.

Even though the classical dynamics for the system studied here is integrable, the semiclassical sum exposed a rich and intriguing interplay between the classical and quantum systems as the wave packet evolves. The classical-path representation examined here has been applied previously to nonintegrable systems, such as the diamagnetic Kepler problem, for short times only. These systems are currently of interest for the implications they carry for the meaning of the correspondence principle. A reexamination of these problems in light of the results presented here promises to be fruitful for further clarification of the classical limit of microscopic quantum mechanical systems.

[1] G. Alber and P. Zoller, Phys. Rep. **199**, 231 (1991).
[2] J. Parker and C. R. Stroud, Jr., Phys. Rev. Lett. **56**, 716 (1986).
[3] G. Alber, H. Ritsch, and P. Zoller, Phys. Rev. A **34**, 1058 (1986).
[4] A. ten Wolde, L. D. Noordam, A. Lagendijk, and H. B. van Linden van den Heuvell, Phys. Rev. Lett. **61**, 2099 (1988); J. A. Yeazell, M. Mallalieu, J. Parker, and C. R. Stroud, Jr., Phys. Rev. A **40**, 5040 (1989).
[5] J. A. Yeazell, M. Mallalieu, and C. R. Stroud, Jr., Phys. Rev. Lett. **64**, 2007 (1990); D. R. Meacher, P. E. Meyler, I. G. Hughes, and P. Ewart, J. Phys. B **24**, L63 (1991).
[6] J. A. Yeazell and C. R. Stroud, Jr., Phys. Rev. A **43**, 5153 (1991).
[7] J. Wals, H. H. Fielding, J. F. Christian, L. C. Snoek, W. J. van der Zande, and H. B. van Linden van den Heuvell, Phys. Rev. Lett. **72**, 3783 (1994).
[8] J. A. Yeazell and C. R. Stroud, Jr., Phys. Rev. A **35**, 2806 (1987); Phys. Rev. Lett. **60**, 1494 (1988).
[9] Z. D. Gaeta, M. Noel, and C. R. Stroud, Jr., Phys. Rev. Lett. **73**, 636 (1994).
[10] Z. D. Gaeta and C. R. Stroud, Jr., Phys. Rev. A **42**, 6308 (1990).
[11] M. Nauenberg, Phys. Rev. A **40**, 1133 (1989).
[12] I. Sh. Averbukh and N. F. Perelman, Phys. Lett. A **139**, 449 (1989).
[13] I. M. Suarez Barnes, M. Nauenberg, M. Nockelby, and S. Tomsovic, Phys. Rev. Lett. **71**, 1961 (1993).
[14] M. Mallalieu and C. R. Stroud, Jr., Phys. Rev. A **49**, 2329 (1994).
[15] M. Mallalieu and C. R. Stroud, Jr. (unpublished).
[16] N. F. Scherer *et al.*, J. Chem. Phys. **95**, 1487 (1991); **96**, 4180 (1992).
[17] J. F. Christian, B. Broers, J. H. Hoogenraad, W. J. van der Zande, and L. D. Noordam, Opt. Commun. **103**, 79 (1993).
[18] L. D. Noordam, D. I. Duncan, and T. F. Gallagher, Phys. Rev. A **45**, 4734 (1992).
[19] R. R. Jones, C. S. Raman, D. W. Schumacher, and P. H. Bucksbaum, Phys. Rev. Lett. **71**, 2575 (1993).
[20] G. Alber, Z. Phys. D **14**, 307 (1989).
[21] S. Tomsovic and E. J. Heller, Phys. Rev. Lett. **67**, 664 (1991); Phys. Rev. E **47**, 282 (1993).
[22] V. P. Maslov and M. V. Fedoriuk, *Semiclassical Approximations in Quantum Mechanics* (Reidel, Boston, 1981).
[23] J. B. Delos, Adv. Chem. Phys. **65**, 161 (1986).
[24] M. L. Du and J. B. Delos, Phys. Rev. A **38**, 1896 (1988); **38**, 1913 (1988).
[25] E. B. Bogomolny, Pis'ma Zh. Eksp. Teor. Fiz. **47**, 445 (1988) [JETP Lett. **47**, 526 (1988)].
[26] J. A. Yeazell, G. Raithel, L. Marmet, H. Held, and H. Walther, Phys. Rev. Lett. **70**, 2884 (1993).
[27] B. M. Garraway, B. Sherman, H. Moya-Cessa, P. L. Knight, and G. Kurizki, Phys. Rev. A **49**, 535 (1994).
[28] M. V. Berry, Proc. R. Soc. London, Ser. A **392**, 45 (1984).
[29] R. G. Littlejohn, Phys. Rev. Lett. **61**, 2159, (1988).
[30] Y. Aharonov and J. Anandan, Phys. Rev. Lett. **58**, 1593 (1987).
[31] J. A. Cina, Phys. Rev. Lett. **66**, 1146 (1991).